

DEUTSCHES ELEKTRONEN-SYNCHROTRON **DESY**

DESY 88-161
November 1988



Tracking in a High Multiplicity Environment

J.B. Dainton

Dept. of Physics, Oliver Lodge Lab., Univ. of Liverpool, UK

ISSN 0418-9833

NOTKESTRASSE 85 · 2 HAMBURG 52

DESY behält sich alle Rechte für den Fall der Schutzrechtserteilung und für die wirtschaftliche Verwertung der in diesem Bericht enthaltenen Informationen vor.

DESY reserves all rights for commercial use of information included in this report, especially in case of filing application for or grant of patents.

**To be sure that your preprints are promptly included in the
HIGH ENERGY PHYSICS INDEX,
send them to the following address (if possible by air mail) :**

**DESY
Bibliothek
Notkestrasse 85
2 Hamburg 52
Germany**

Tracking in a High Multiplicity Environment

J B Dainton
Department of Physics
Oliver Lodge Laboratory
University of Liverpool, P O Box 147, Liverpool L69 3BX, UK

1 Introduction

In the last 10 or 15 years the case for charged track reconstruction in both fixed target and modern collider experiments (e^+e^- , pp and ep) has been overwhelming. Despite increasing difficulty due to the worsening complexity of the final state topology with associated increases in centre of mass energy, the reasons for charged track detection have, if anything, become both more persuasive and more numerous. Though the best argument for tracking is to imagine data from one's experiment without it, it is nevertheless worth attempting to list these reasons:

1. measurement of charged multiplicity;
2. measurement of jet fragmentation multiplicity and kinematics about the jet axis;
3. accurate determination of event vertex(ices);
4. beam gas and multiple beam vertex rejection;
5. π/e separation in a downstream calorimeter by geometrical association of energy cluster and track or jet;
6. study of calorimeter response;
7. accurate measure of p_T ;
8. charge of secondaries;
9. further enhancement of π/e discrimination using reconstructed momentum;
10. μ identification;
11. energy dependence of calorimeter response.

Items 1 through 6 do not require any magnetic field, items 7 through 11 do. Most experiments consider the latter as well worth the added complication of a magnet and some studies at future ultra-high energies even suggest that track reconstruction may only be possible with the spreading of high p_T tracks and removal of confusing low p_T tracks in an axial magnetic field. Fixed target experiments use large dipole magnets to produce magnetic fields transverse to the incident beam direction. All but one collider experiment (UA1) which include charged track momentum reconstruction have chosen axial (solenoid) magnetic fields.

In this presentation I want to try and highlight some of the features, both similar and dissimilar, of charged track detectors, all of which by default operate in a high multiplicity environment, generically referred to as "inner tracking", "central tracking" or "vertex detectors" in collider geometries, and as "spectrometers" in beam target configurations. I will restrict myself to gaseous detectors. Other techniques are well covered elsewhere at this conference [1]. I will also attempt to emphasise the relevance of some of these features to detectors at the next generation of high energy colliders, namely SSC, LHC, and CLIC.

Large track multiplicity influences design of gaseous detectors in two major ways. Firstly, the effect of high occupancy in a drift cell limits the useful operation of proportional wires both instantaneously due to gain sag at high rate because of electrostatic shielding of the sense wire avalanche field, and in the long term by shortening chamber lifetime because of deposition on the sense wires of di-electric material from C-crack reactions or from impurities in the chambers and infrastructure, usually Si [2]. The lifetime of sense wires is essentially determined by the total ionisation charge collected - the rule of thumb critical limit is ~ 1 C/cm wire. Secondly, the effects of track overlap within the chamber volume lead directly or indirectly (through pattern recognition confusion) to loss of track point data with all its obvious drastic consequences. Track overlap problems are best solved by built-in redundancy in detector configuration, by space point read-out wherever possible with the best possible precision, and by the best two track resolution in both space point co-ordinates. Both of these problems are further compounded by the presence of photon conversions in the concomitant high neutral multiplicity always present, and by machine background - synchrotron and "beamstrahlung" radiation from electrons, and beam halo, including penetrating muons, from protons.

Time and space are perforce limited and so I cannot hope to be fair to others and include all of the immense amount of work that has gone into the past and present generations of charged track detectors. The priority here must be to cover the papers submitted to this conference, placing them in the broader context of some of the more noteworthy features of all present and future gaseous charged track detectors.

Tracking in a High Multiplicity Environment

J B Dainton
Department of Physics
Oliver Lodge Laboratory
University of Liverpool, UK

Abstract

An attempt is made to highlight and contrast some of the features of present charged track detection in both collider and fixed target experiments using gaseous drift chambers. New examples of such detectors, presented at this conference, are summarised in the context of other contemporary work. Brief consideration is given to how experience with present day detectors may contribute to the possibilities for charged track detection at future super-colliders.

Based on a "Mini-rapporteur" talk in Parallel Session 22
"Detectors in High Energy Physics"
at the XXIV International Conference on
High Energy Physics, Munich, FRG, August 1988.

(Abridged version published in the Proceedings of the conference.)

In all discussion I will take the beam axis to be z and transverse co-ordinates to be (r,φ) or (x,y). φ is the usual spherical polar angle (arctan r/z).

2 Contemporary Charged Track Detectors

2.1 Time Projection Chambers

Over a large solid angle the Time Projection Chamber (TPC) provides redundancy and spatial precision with few wires and over a large angular range [3]. It does so by exploiting the uniformity of magnetic field B in large volume solenoids and dipoles where drift over long distances parallel to B is not hampered by ExB effects.

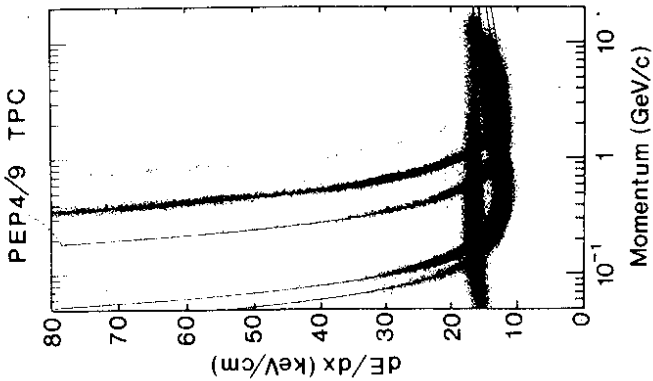
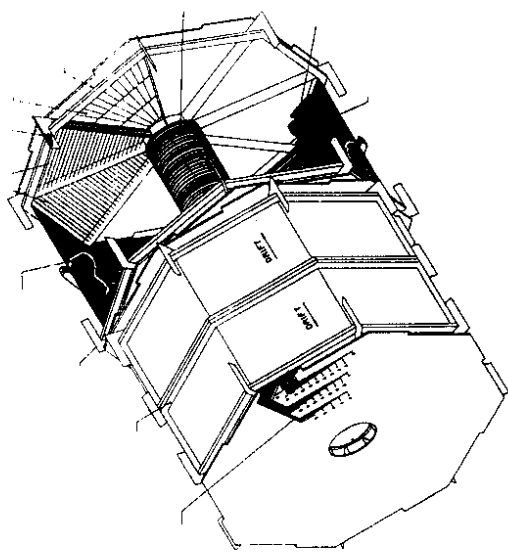


Fig 2. Measurement of dE/dx of charged tracks from e+e- interactions reconstructed in the TPC of the PEP4 experiment at SLAC [7].

Fig 1 shows both the schematic construction of the CDF vertex TPC (VTPC) and how it handles 1.8 TeV pp interactions at the Fermilab collider [4]. Two interactions are visible in this bunch crossing and this detector, which is actually the inner, most "upstream", gaseous track detector, clearly resolves well the event topology. The spatial resolutions achieved are in r-z (200 to 500 μm, max drift length 15 cm) and in r-φ (300 μm/cm track), and the 24-fold sense wires and associated cathode pads are seen to provide adequate precision and redundancy to resolve typical event topologies (mean charged multiplicity 26) over the angular range 3.5° < φ < 176.5°. The detector itself is a very lightweight construction of kapton/rohacell laminate with carbon fibre support ribs and so contributes minimally to degradation of downstream calorimeter resolution and to photon conversion (~2% radiation length at θ ~ 90°).

The much larger LEP TPCs, at ALEPH [5] and DELPHI [6], can thus be expected to perform spectacularly next year. Prototype tests have shown that they will yield spatial resolution similar to the CDF VTPC per track point. Operation in strict proportional mode plus their much larger dimension, and thus much larger number of track points, will also yield useful dE/dx particle identification. The first TPC at PEP4 tells us that with great style [7], albeit at 8 bar gas pressure (fig 2), and at this conference we have seen beautiful new physics from its clone, the TOPAZ TPC at TRISTAN [8].

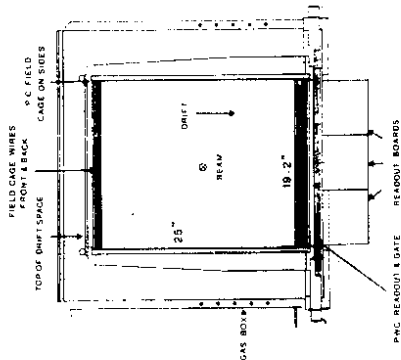


Fig 3. Schematic construction details of the anode read-out TPC modules in the Brookhaven MPS heavy ion experiment; also shown is the anode read-out structure [9].

There are other places where severe multi-track environments can be found and TPCs are now being used successfully. At this conference an anode read-out TPC is reported for relativistic heavy ion physics at Brookhaven, more particularly for a quark-gluon plasma search and its anomalous yield of p/A plus possibly additional Vs [9]. Everything is of course rotated relative to the heavy ion beam to match the Brookhaven Multi-Particle Spectrometer (MPS) dipole magnet so that drift is vertical (y parallel to B) and the incident beam passes through the centre of the TPC. The TPC module is a very

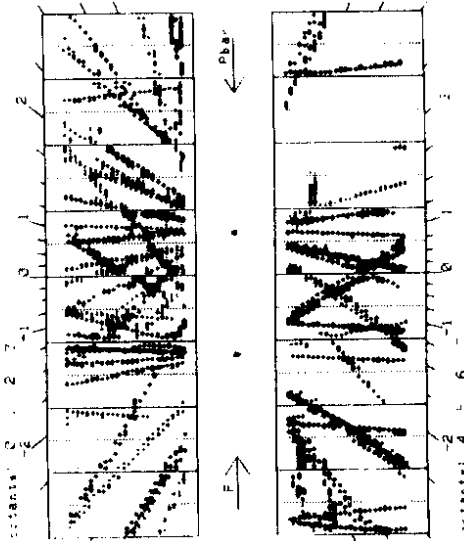


Fig 1. Schematic of the construction of the vertex TPC in the CDF detector at the Fermilab collider, and r-z event display of two simultaneous 1.8 TeV pp interactions [4].

straightforward, and cheap, device (fig 3). Read-out of fully 3D space points is by means of the usual drift measurement (y) to short (1 cm) sense wires. The latter are aligned along z, are grouped in bands in z, and are spaced out in x across the transverse dimension of the chamber (10 wires/inch). The use of such wires, rather than a pad system as in the original collider TPCs, has one disadvantage, namely that it is impossible to maintain adequate uniformity of gas gain along the length of each wire for dE/dx measurement.

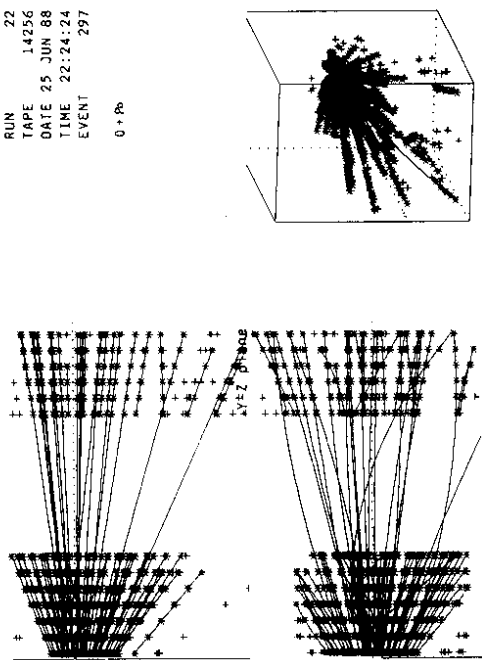


Fig. 4. 80-prong event produced by 14.5 GeV/c oxygen ions incident on a lead target in the Brookhaven MPS heavy ion experiment; first attempts at event reconstruction are superimposed [9].

Four such TPC modules will be situated in the MPS magnet. A high gain gas (Ar:isobutane i-C₄H₁₀ with methylal) means that good two-track separability of 2 to 3 mm is achieved over a maximum drift length of 0.64 m. Space point resolution is better than 1 mm in both co-ordinates perpendicular to the incident beam (x from the short sense wires and y from drift time). In π and p beam events > 90% track reconstruction efficiency is achieved, and, most impressive of all, the group has just taken first test data with 14.5 GeV/c O on a thin Pb target (fig 4) and handled secondary multiplicities of ~80 with ~75% efficiency when the beam rate is a few times 10³ O sec⁻¹. With the availability of the booster at the AGS and the advent of Au (golden!) beams, it may be necessary to deaden the beam region of each module and this is anticipated in the design.

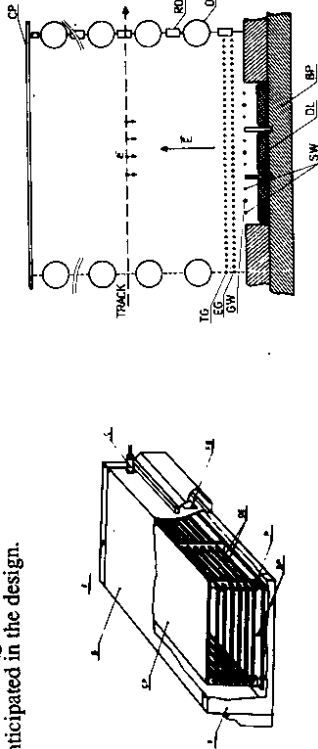


Fig 5. Schematic of the Dubna/Tashkent TPC with delay line read-out; B - container, F - endcaps, C - HV connector, BP - base plate, DE - field forming electrodes, P - fibreglass frames, CP - cathode plane, FB - electronics [10].

A Dubna/Tashkent group have presented to this conference the results of the construction and testing of a TPC (fig 5) with electromagnetic delay line read-out for use in fixed target experiments, in particular

precision measurements of K⁺ decay and study of the ppy system in π C interactions [10]. Two transverse co-ordinates of a track are measured using the ionisation drift time measurement and delay lines parallel to each sense wire. The drift time resolution is as expected (300-500 μ m in Ar:i-C₄H₁₀ 83:17) when compared with other TPCs, and the authors quote a minimum adjacent track separation in this co-ordinate of at least 4.2 mm. The delay line replaces the more conventional cathode pad structure and a resolution of ~3 mm is obtained, again very similar to pad read-out in other TPCs. The group estimates a minimum two-track resolution of 42 mm in this co-ordinate.

Both these fixed target experiment TPCs compare well with that in the NA36 heavy ion experiment at the CERN SPS which has now taken data [11]. The experiment ran with the TPC to one side of the target. Fig 6 shows impressively the power of TPC 3D space point detection in higher energy 200 GeV/nucleon heavy ion physics.

All in all, after Nygren's pioneering work at SLAC, TPC technology is now coming to fruition in a most spectacular way.

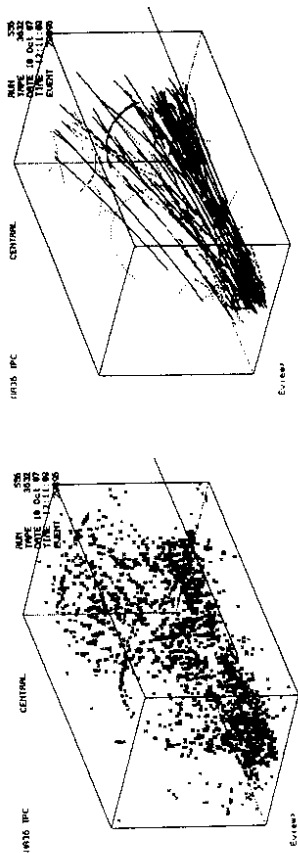


Fig 6. Heavy ion interaction in the CERN NA36 experiment TPC; also shown are the reconstructed tracks in the event [11].

2.2 Multi-cell Central Drift Chambers

Most recently Saxon has succinctly traced the evolution of what has become the approach alternative to a TPC, the multi-cell drift chamber [12].

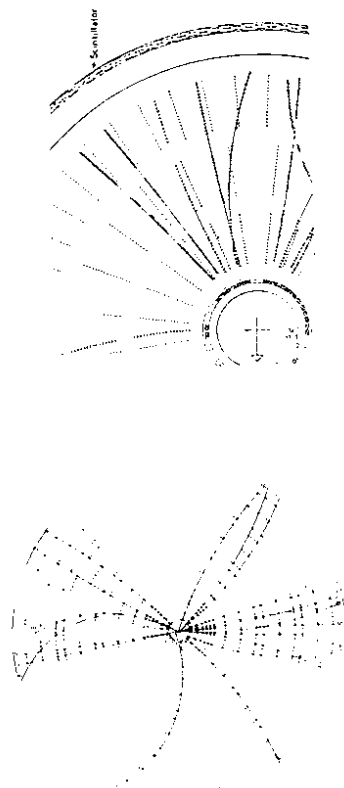


Fig 7. Typical e⁺e⁻ events in the TASSO central detector and in the JADE jet chamber at the PETRA storage ring.

track crossed many single wire cells and the associated random redundancy covered for the inevitable multi-occupancy of some cells by adjacent tracks. The z co-ordinate was determined with two different stereo tilts on different cells ($\sigma_z \sim 3$ mm). In the latter case multi-hit electronics at each end of the sense wires yielded a high density of hits in each multi-wire drift cell. These are resolved into space points by small individual sense wire stagger (~ 100 μ m) and by charge division ($\sigma_z/z \sim 1\%$). In both cases the benefit of good drift measurement accuracy ($\sigma \sim 100$ - 200 μ m), even with operation in magnetic fields of ~ 0.5 T, ensured the required momentum resolution.

Comparison of the performance of each solution is illuminating. In the multi-cell, single wire, device the redundancy may not overcome the severe drawback of single hit read-out so that track following becomes derailed. Particle identification by dE/dx is difficult because the track length within a cylindrical cell may vary greatly. In the JADE multi-wire cell device long segments of tracks can be lost due to tracks adjacent in (r, ϕ) and yet far apart in z (fig 7), and the relatively poor precision in z compounds resultant ambiguities, so much so that in later running JADE installed an outer z chamber in which axial drift (along the direction of B) to cylindrical wires gave good z resolution.

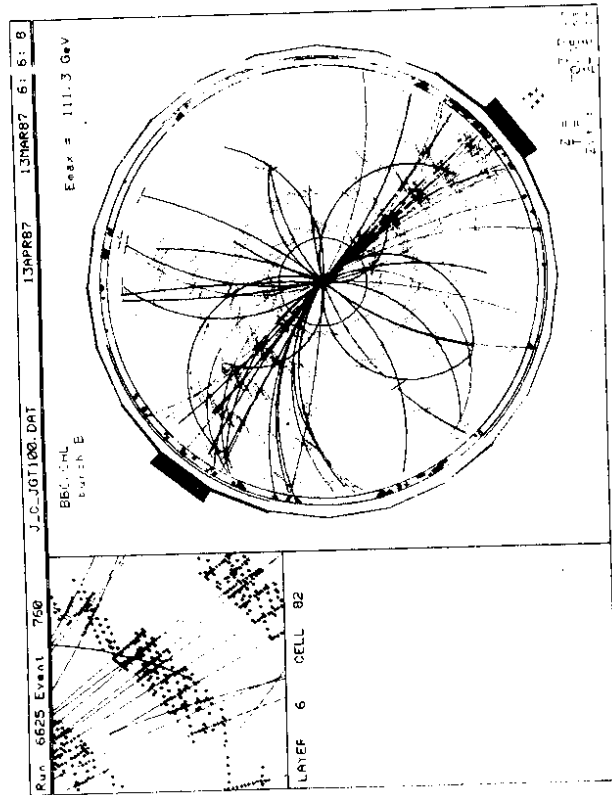


Fig 11. r - ϕ views of early CDF data including a blow-up of part of the tracking, showing that the efficient rejection of ghost track segments is unambiguous [4].

The MarkIII central drift chamber at SPEAR [14] followed by the MarkII upgrade for SLC [15] made the first attempts to combine the advantages of single wire and multi-wire cell devices discussed above. Layers of jet chamber-like cells, some with stereo angle (usually in such chambers between 3° and 7°), are staggered relative to each other (MarkII in fig 9). Each cell thus provides a track segment or "vector" for track following rather than just a point, the segment redundancy is large (~ 80 layers between inner and outer radius), and each track crosses cells with very different drift lengths (maximum drift length can vary between ~ 25 and 35 cm) and always in some cells crosses the sense wire plane, thereby providing an absolute drift "t₀" determination on every track. Saxon aptly calls such devices "stereo superlayer chambers" (SSCs) [12]. When in the MarkII coil ($B = 0.5$ T) the cells are operated with a Lorenz angle of 19° so that the accuracy in the high precision drift measurement is no longer completely in the wanted $r\phi$ direction.

Meanwhile at LEP, as we have seen, the influence of the successful TPC at PEP has been great. Only OPAL opted for a multi-cell device [13]. It is obviously a development of the successful JADE chamber, filling the cylindrical volume about the beam pipe ($\phi = 0.5$ m) to a diameter of 3.7 m with 24 jet

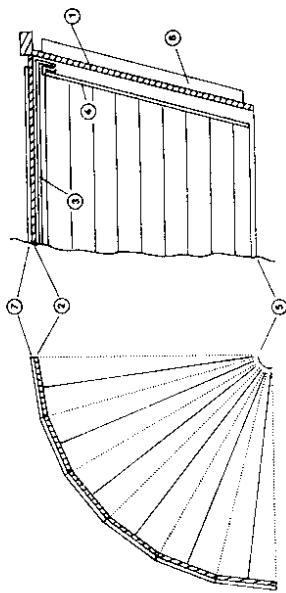


Fig 8. Cross sections through one quadrant of the final OPAL jet chamber viewed in the r - ϕ and r - z planes. The cathode and sense wire planes, the conical end-plate (1), the shell of aluminium panels (2), barrel (3) and endcap (4) field shaping electrodes, inner field shaping (5), the anode wire suspension (6) and the z chambers (7) are indicated [13].

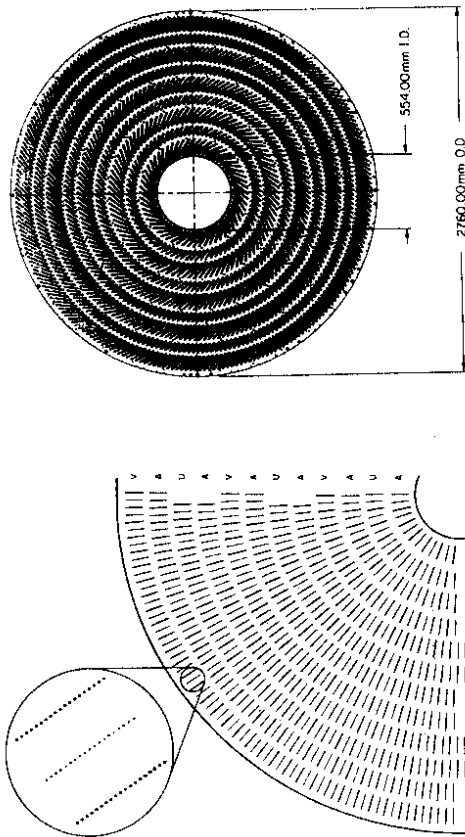


Fig 9 Configuration of wire support holes in the end-plates of the CDF track detector; the tilted drift cells for compensation of the Lorenz angle and for at least one fast signal per reconstructable track are apparent [4].

Fig 10 Configuration of wire support holes in the end-plates of the MarkII central detector at SLC; stereo superlayers are marked U and V; each superlayer contains 6 sense wires [15].

The original "central detectors" of MarkII at SPEAR and PLUTO at DORIS used spark and proportional chambers with relatively low point density and with (nowadays) poor precision. The problems of track overlap with the increase in multiplicity at PETRA and PEP were solved in one of two ways. The first was by means of the redundancy of large numbers of small, cylindrical, randomly arranged, single wire drift cells with single hit read-out (MarkII, and later TASSO, PLUTO, CELLO, CLEO and ARGUS), and the second used an assembly of independent, multi-wire drift cells with multi-hit read-out per wire and relatively long drift lengths (JADE jet chamber) (fig 7). In the former case each

Their radii are chosen to ensure good z measurement on tracks with $\theta < 30^\circ$ and thereby to guarantee good matching of tracks in the central and forward track detectors (see section 2.3 below and fig 20). Each z chamber consists of cells containing four sense wires strung polygonally round the beam. Ionisation drift is axial and therefore parallel to B. Several such cells with maximum drift lengths of 60 mm (CIZ) and 46 mm (COZ) in z complete the full axial length of the CTD. H1 also include trigger multi-wire proportional chambers sandwiching CJC1, CIZ and COZ which guarantee fast signals (within 96 ns) from all interesting events.

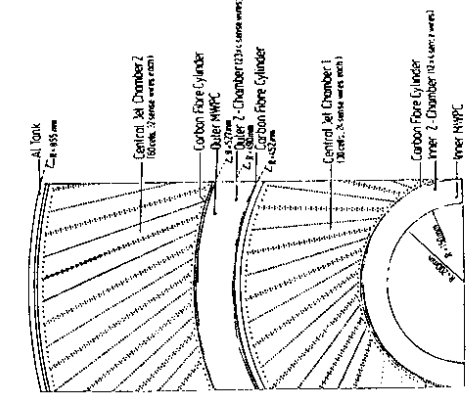


Fig 13 r-phi view of the H1 central track detector (CTD) showing the geometrical arrangement of the CJC1 and CJC2 jet chambers. CJC1 is sandwiched by inner and outer z chambers and by MWPC trigger chambers [19,20].

Fig 14 Drift cell (r-phi view) of an H1 CJC showing the isochronous contours in the tilted CJC1 and CJC2 jet chambers. Also shown is the double plane of field (potential) wires to reduce cross-talk to minimise surface fields and to make for better cell isochronicity [19,20].

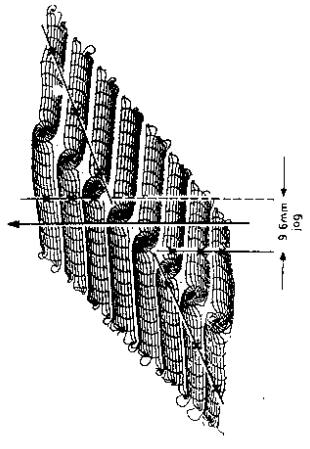


Fig 15. Simulated digitisations and parent tracks in a Zeus and H1 cell showing how a background track from an earlier HERA bunch crossing fails to produce a collinear track segment [12,19]. It is no accident that 2 out of 3 experiments with axial magnetic field at LEP chose TPC detectors and 2 out of 2 at HERA chose multi-cell drift chambers. The HERA experiments have to live with an inter-

chamber multi-wire cells (fig 8). The cell design involves 159 axial sense wires per cell distributed radially together with their bounding cathode wire planes. The drift length ($r\theta$) varies between 3 cm at the inner radius and 25 cm at the outer radius and is operated at 4 bar overpressure to achieve a point resolution in the drift measurement of $r\theta$ of between 100 μm and 220 μm over the cell. Such a device exploits naturally FADC read-out on both ends of each sense wire and thereby, with the associated software overhead, is able to achieve simultaneously good timing, charge division and pulse integral analysis. The high pressure operation (gas gain 10^4) with a maximum of 159 sense wire samples ensures excellent dE/dx particle identification. An outer z chamber is also included.

The significantly higher multiplicities in Lorenz boosted jets at the HERA and Tevatron colliders call for another step forward in the stereo superlayer concept. To achieve the necessary momentum resolution ($\sim 0.3\% \text{ GeV}^{-1}$) with typical multi-wire cell point resolution ($\sigma_{\text{drift}} \sim 100 \mu\text{m}$), solenoid fields of $\sim 1.2 \text{ T}$ or more are necessary. CDF [4], followed later by Zeus at HERA [12,16], then minimise the effects of the substantial Lorenz angle by tilting the sense wire planes relative to the radius vector so that the actual ionisation drift remains still roughly a measure of $r\theta$ (fig 10), but one cannot now work with either polarity of solenoid magnetic field). There are then other advantages:

- i) many more tracks cross a sense wire plane many times, thereby further facilitating calibration of, and adjacent track distinction in, the drift cells, and making triggering from drift chamber data possible, and
- ii) resolution of left-right drift ambiguity, that is removal of "ghost" track segments, becomes trivial.

Fig 11 shows early CDF data in such a chamber, including fitted tracks and ghost hits. The power of track following between vector segments is apparent. It is also very fast computationally, involving only bilinear products of segment parameters to test for an acceptable orbit in the $r\theta$ bending plane. This makes it realistic to conceive of fast microprocessor controlled front-end filtering, something which is more and more important in high rate colliders.

The Zeus superlayer chamber has also to accommodate the asymmetric HERA kinematics (30 GeV e on 820 GeV p) which, as discussed in section 2.3 below, tends to throw tracks into the forward proton hemisphere. The group is thus investigating timing as a means of z determination with inner axial sense wires [17]. The hopes are to be able to derive a fast forward charged track trigger and to help in the reconstruction of steep forward tracks which do not make it to the first stereo layers. The aim is for a resolution $\sim 3 \text{ cm}$ that is an accuracy of 200 ps in a time difference of $\pm 8 \text{ ns}$. Fig 12 shows the first encouraging attempt with electronics not yet optimised in which ionisation signal to noise limitation is apparent.

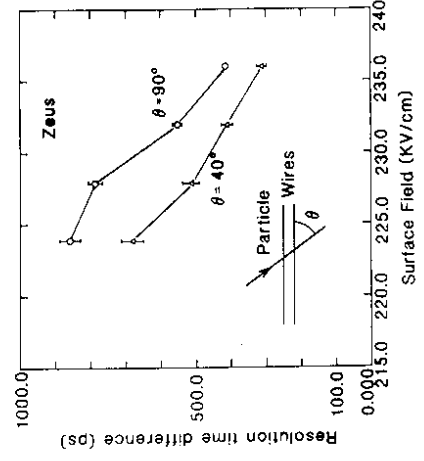


Fig 12. Precision of z co-ordinate in the Zeus CTD determined by timing difference between each end of sense wires [17].

Such timing techniques are well proven on sense wires operated in limited streamer mode where the absence of any need for preamplification of the large primary pulses means that excellent resolution ($\sim 3 \text{ mm}$ in 4 m), limited by noise in the sense wire and by the quality of comparator electronics and cable, is possible [18]. The attempt by Zeus with sense wires in proportional mode is, with optimised electronics and cable, ultimately limited in its resolution by a straight compromise between adequate gas gain for good pulse signal to noise and low enough gas gain for the chamber to survive in HERA.

The central tracking detector (CTD) for the H1 experiment at HERA follows more closely the philosophy of JADE and OPAL [19,20]. The basic multi-wire drift cell structure is just two layers (CJC1, CJC2) of OPAL-like jet chamber cells (24 and 32 sense wires per multi-wire cell) but tilted at 30° for the same reasons as CDF and Zeus (fig 13). Unlike the OPAL chamber, the H1 drift cells employ double potential wires (fig 14) so as to halve the sense wire cross talk and reduce surface fields. Such double potential wire configurations also enhance both isochronicity and two-track separation in the cell. Charge division provides a z measurement for space point reconstruction. To enhance the z resolution two cylindrical z chambers are included sandwiching CJC1 at radii of 200 mm and 470 mm.

ep collisions means that forward track detection is necessary (see section 2.3 below) and H1 has made some effort to design lightweight end-plates using 10 mm glass fibre reinforced epoxid (G10). The resultant wire support in the end-plate is shown in fig 18 [19,20].

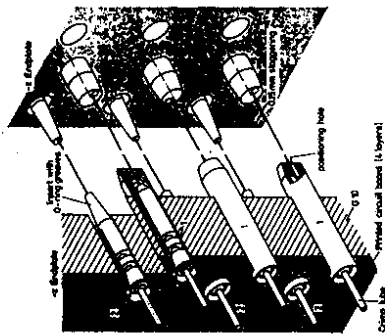


Fig 18. Wire fixation by means of feed-throughs and crimps in the end-plates of the H1 C/JCs [19,20].

HERA ep 30 GeV • 820 GeV s = 98400

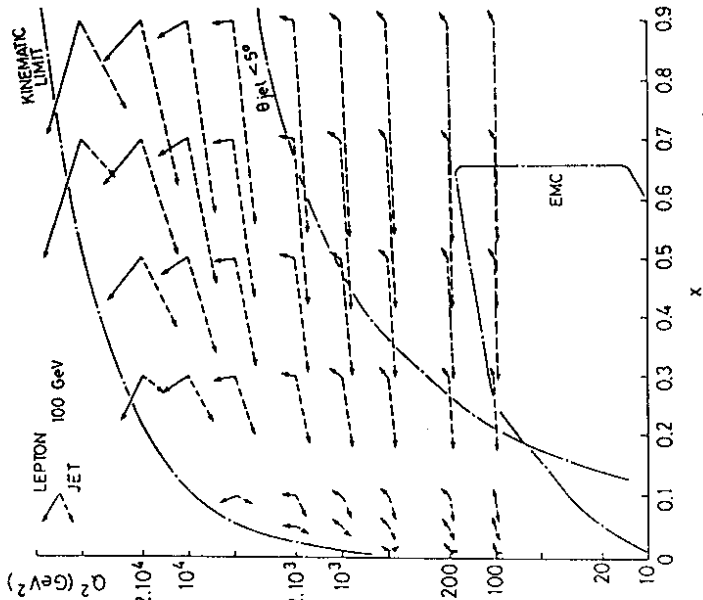


Fig 19. Scattered lepton and (massless) parton vectors in standard model events as a function of x and Q^2 at HERA. For high mass excitation of the parton current, the parton vector is at even smaller angles to the incident proton beam than shown.

bunch crossing time of 96 ns, a sign of things to come at LHC or SSC, which completely precludes the operation of conventional TPCs with large maximum drift times. Nevertheless the magnitudes of the maximum drift times in the H1 and Zeus designs (1500 ns and 500 ns respectively) are equivalent to many bunch crossings so that data must be read-out into pipelines which are strobed after time sufficient for trigger decision logic has elapsed. Both experiments rely on their tilted drift cells and the fact that tracks will always cross a sense wire plane to eliminate out of time (late by multiples of 96 ns) track segments within a cell (fig 15), but H1 also have the fast inter-bunch read-out of the inner and outer MWPCs (fig 13).

The CDF, H1, MarkII and Zeus chambers are designed to operate with drift fields of between 1 and 1.6 kV/cm and gas mixtures (Ar:C₂H₆:50:50, Ar:CO₂:CH₄:89:10:1 (HRS) gas [21]) which have a drift velocity ~50 μm/ns. With 100 MHz flash ADC read-out giving, by means of software pulse shape analysis, ~2 to 3 ns timing resolution (H1, Zeus), or with 2 ns TDC read-out (MarkII), these detectors guarantee ~100 μm point resolution at small drift distance which is still electronics limited.

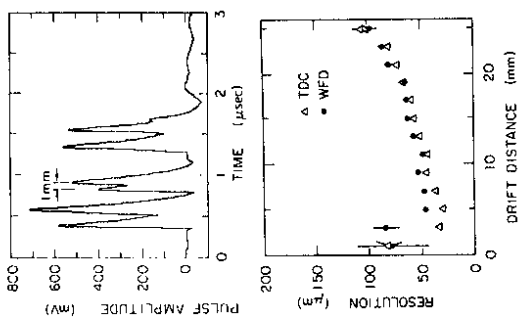


Fig 17 a) Multi-track event in the SLD inner detector prototype showing excellent (1 mm) track separation achieved with a slow gas and an optimised drift cell, and b) position resolution as a function of drift time using two different sets of read-out electronics [22].

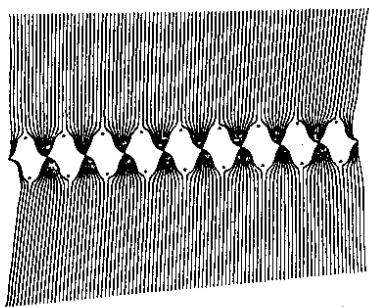


Fig 16 SLD prototype drift cell including the calculated electron drift trajectories in a magnetic field B of 0.6 T [22].

The central multi-cell chamber currently under construction for SLD is a little different [22]. It uses a slow gas (CO₂ and i-C₄H₁₀ mix) with an unsaturated drift velocity ($v_{drift} \propto E_{drift}$) of ~9 μm/ns. The (by now) somewhat familiar drift cell includes the double potential wires also found in H1 (fig 15) in which considerable focusing occurs near the sense wire plane. The result is to separate somewhat the drift region from the avalanche region and thereby improve the isochronicity throughout the cell. Not only is the point resolution improved ($\sigma_{drift} < \sim 50 \mu m$ - because of both slower drift velocity and less diffusion), but also, with FADC read-out, the two-track separation can be as small as 1 mm, albeit with a slightly higher gas gain (~10⁵) than in other multi-cell detectors (fig 16). With such excellent spatial precision throughout such a large central detector, calibration and monitoring become extremely tricky.

The method of construction of multi-cell devices like those above is in essence the same. Wire positioning accuracy is achieved by precision machined end-plates which also provide mechanical stability against axial (z) wire tension (e.g. 25 tonnes in CDF [4]). There are some differences between wire fixation - crimp pins in feedthroughs, combs and solder, etc., and most detectors claim an accuracy in wire position of 10 μm wire to adjacent wire on a comb or equivalent and <~25 μm between groups of wires on different combs. Wire tensions are chosen for minimal and similar gravitational sag on all wires (e.g. ~200 μm in OPAL [13]) irrespective of diameter. At HERA the asymmetric kinematics of the

efficiency for charged tracks down to $\theta \sim 5^\circ$ but with the consequential loss of momentum resolution at ϕ values along the direction of B . The asymmetric e^+p kinematics at HERA (30 GeV/c electrons on 820 GeV/c protons) boosts many fragments into the forward proton direction even at substantial Q^2 (lepton P_T) (fig 19 and fig 20 b)). Both HERA experiments, H1 and Zeus, therefore include additional charged track detectors in the forward (proton) direction, called forward track detectors (FTD), to enhance the coverage of their central tracking down to a polar angle $\theta \sim 5^\circ$ [16,19,20].

In H1 (and, though not shown here, also in Zeus) the CTD extends in z until $\theta \sim 30^\circ$ at maximum radius (figure 20 a)) [16,19,20]. For tracks at smaller θ the space point precision obtained with the axial (z) wires in a multi-cell drift chamber CTD (as discussed above) deteriorates seriously. So both experiments have FTDs which include arrays of drift chambers with wires strung perpendicular to z . Perhaps surprisingly in an axial (i.e. solenoid) magnetic field, it is possible with a realistic array of such chambers to achieve an adequate density of track points when projected into the r - ϕ (bending) plane so as to compensate for the reduced track length at small θ (fig 21). Thereby both the required momentum resolution and the multi-track pattern recognition can be maintained to smaller θ .

The H1 FTD includes radial wire and planar drift chambers for efficient multi-track reconstruction, together with MWPCs for fast timing and transition radiators to enhance electron identification by pulse height analysis (fig 20). The radial drift chambers provide the momentum resolution and detect transition radiation (TR) X-rays generated by electrons in the preceding radiators. The planar drift chambers remove certain pattern recognition ambiguities which remain and also make up for the deficit in momentum resolution caused by the lack of track point data in the space occupied by the transition radiators.

The radial wire drift chambers consist of 48 wedge shaped, multi-wire, drift cells, rather like jet chamber cells but with sense wires strung radially and each cell divided with voltage graded cathode strips (fig 22) [20,23,24]. The principle of such chambers was originally proven at CDF where similar devices operate in the extreme forward direction outside the solenoid magnetic field [4,24]. Resistive sense wires in wedges at $\sim 90^\circ$ to each other are connected at the inner hub and are read out at the outer radius of the chamber. Space points are obtained from drift time measurement transverse to the incident particle direction and by means of charge division. Each wedge has 12 sense wires to provide vector track segments. The radial chambers are operated in proportional mode (gas gain $\sim 10^4$) with a gas suitable for the TR X-ray detection (Xe: C₂H₆:He 30:30:40, drift velocity $\sim 28 \mu\text{m/ns}$) on any of the chamber's sense wires. The electrostatics of each wedge, which maintains the transverse drift of deposited ionisation, must therefore guarantee 100% ionisation collection efficiency on each sense wire in a drift cell with no losses to field (potential) wires. The chamber window adjacent to the TR has been carefully designed for maximum X-ray transmission without any significant degradation of this transverse drift spatial precision.

The choices of radial sense wires and solenoid magnetic field in the forward direction are naturally matched. The radial chambers measure $r(\theta)$ (drift) and $\sim r$ (charge division). In a solenoidal field a track trajectory has a linear dependence of ϕ on z so that track segment recognition both within and between radial chambers is very fast. Thus, like the multi-cell drift chambers of section 2.2 above, radial wire drift chambers also have the features of "vector chambers" with the benefits of fast data reduction, possibly in front-end microprocessors.

Despite the conflicting demands on the operating characteristics of the radial chambers due to the simultaneous requirements of good drift time measurement, good charge division and good ionisation statistics, the compromises inherent in the choice of operating conditions seem not to be serious. Fig 23 shows the results both for track point measurement and for η / ϕ discrimination. One may therefore

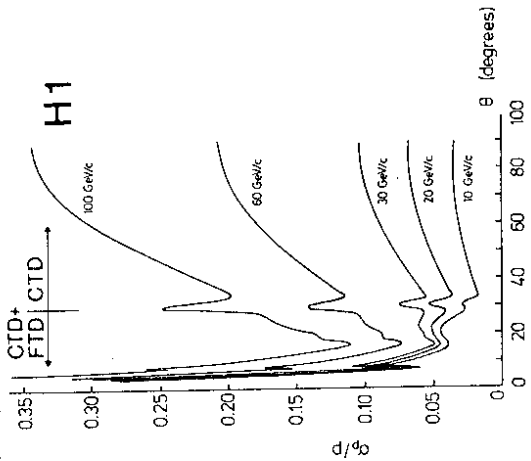


Fig 21 Track momentum resolution as a function of polar angle θ showing the effect of including a forward track detector in an experiment with uniform axial (solenoid) magnetic field (calculation for H1).

The operational performance of multi-cell, central drift detectors compares well with those of TPC-like devices. They yield better ϕ accuracy, good two-track separation, can operate in high bunch crossing rate environments and give rise naturally to very fast first level data reduction suitable for on-line microprocessor filters. Their major drawbacks are in z resolution, which is nowhere near the ~ 0.3 mm of a TPC, and in the very labour intensive technique of construction involving the stringing of very large numbers of wires to within tight mechanical tolerances.

2.3 Forward Drift Chambers

In e^+e^- colliders, with the notable exception of $\gamma\gamma$ physics, the polar angle (θ) coverage of central detectors, such as multi-cell chambers described above, is adequate, and with TPCs is good. In hadron colliders a central detector in a solenoidal magnetic field ensures good coverage over a large part of the P_T region of perturbative physics - e.g. in CDF this includes charged track reconstruction over the pseudorapidity range -3.5 to 3.5 without its very forward chambers which sit outside the solenoid. In contrast UA1 uses a dipole magnetic field and drift chambers with different wire orientations to permit good

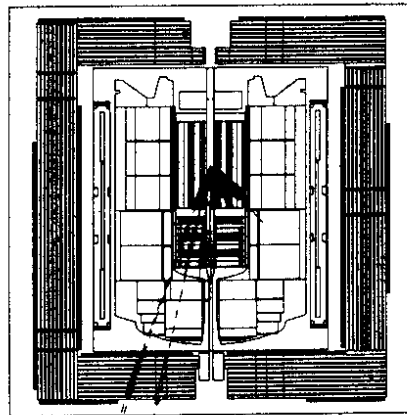
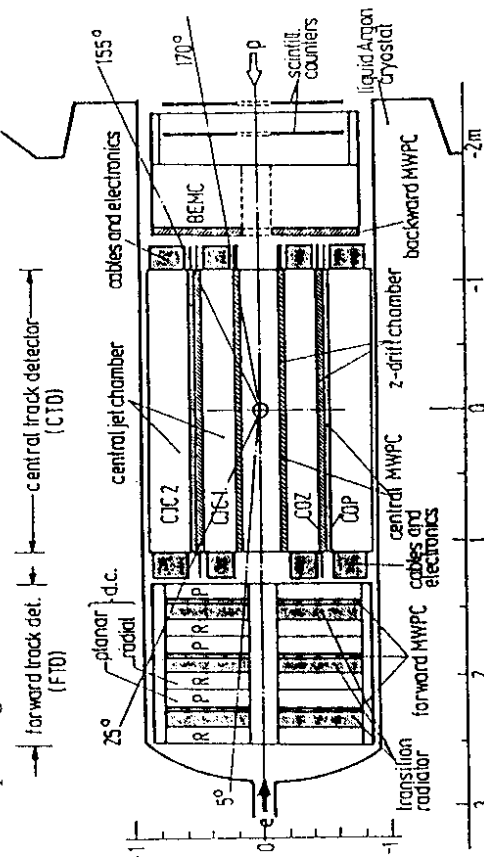


Fig 20 r-z view of the H1 inner track detectors showing the basic elements of the CTD and FTD [19,20], and simulated standard model event in the H1 forward and central track detectors.

anticipate that the H1 FTD not only will extend charged reconstruction down to forward angles, but also will find with good efficiency electrons close to, and may be even inside, jets in this forward region.

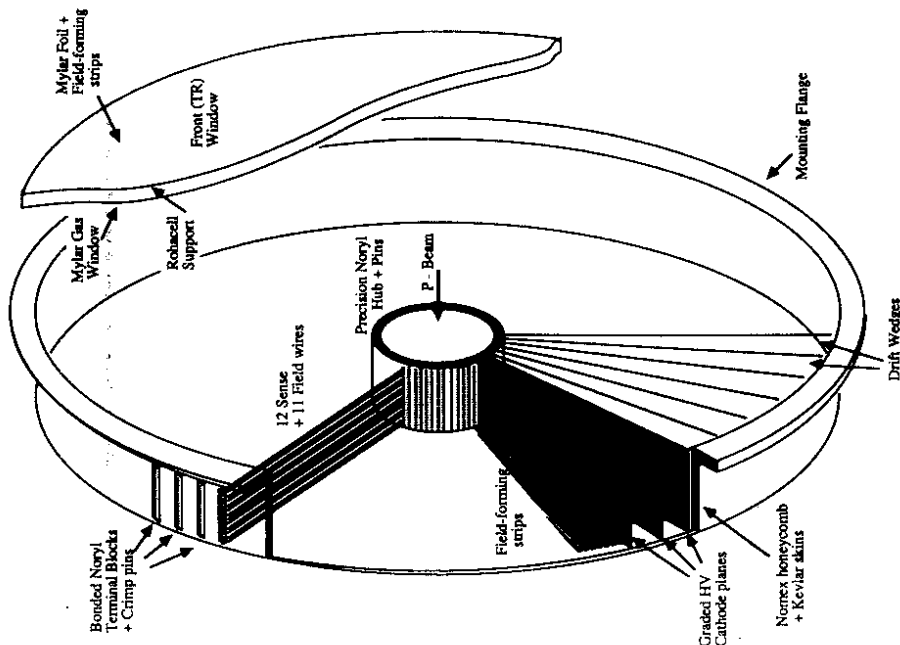


Fig 22. Exploded view showing the principle of construction of a radial wire drift chamber for the H1 FTD. The flat "saucerpan" like structure supports radial wires strung between an inner hub and the outer radius. The upstream window of the chamber is designed to maintain the drift accuracy (transverse to the incident particle) while simultaneously having the best possible X-ray transmissivity for detection of transition radiation.

The H1 FTD is the most ambitious forward track detector at a high energy collider, other than perhaps the UA1 inner detector which extends to similar angles but with a dipole magnetic field geometry. Its feasibility derives in part from the relatively uniform axial (z) magnetic field in this region due to the choice of a large radius solenoid for H1. The Zeus experiment, which has opted for a small radius coil, also includes an FTD, but with a simpler array of chambers and with segregation between those parts optimised for track reconstruction and for TR electron identification [16]. It will be most interesting to see how these FTDs perform in the real world of HERA beams and background!

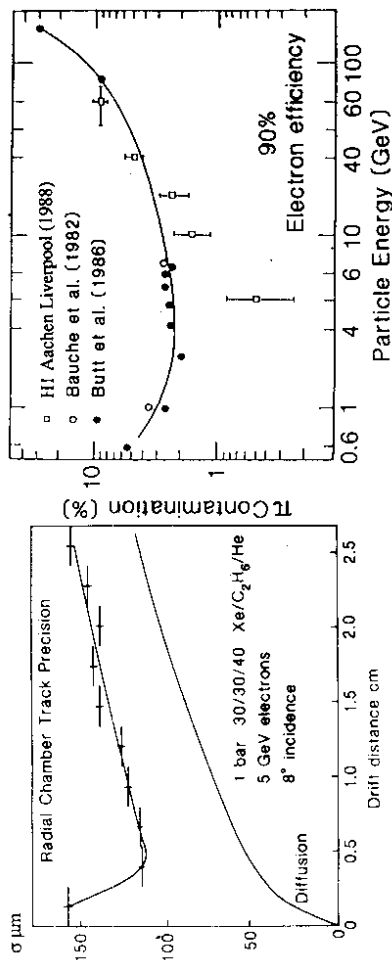


Fig 23. Measurements of the spatial precision and of the e/π discrimination in a radial drift chamber prototype using a dilute Xe based gas mixture suitable for efficient X-ray detection.

2.4 High Precision Vertex Chambers

As already discussed in section 2.2, the use of slow gas (CO₂ and i-C₄H₁₀), careful drift cell design, and accurate and careful construction can provide point accuracy in a drift chamber of 50 μm without resort to over-pressure (fig 17). These techniques have been exploited, together with a high density of drift cells operating close to the primary event vertex, to provide high resolution vertex detectors at LEP and SLC [25]. The motivation is of course to identify heavy quark flavours by means of secondary event vertices.

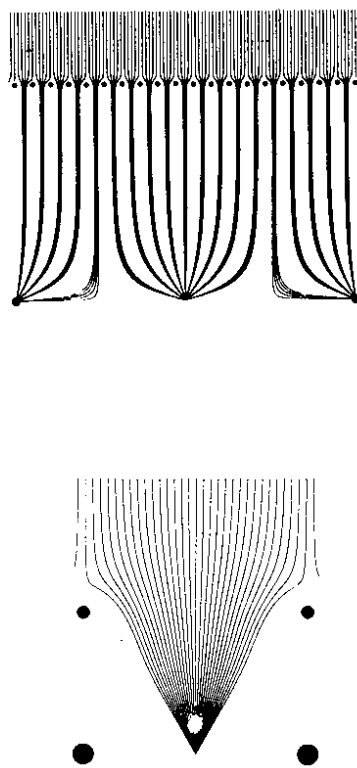


Fig 24. Ionisation drift trajectories in the MarkII vertex detector at SLC and the L3 time expansion chamber at LEP [25].

When over-pressure is combined with a slow gas, measurements of spatial resolution between 20 and 50 μm have been achieved without using special read-out electronics [25]. The drift cell is optimised given the constraints of mechanical stability of the closely spaced wires, sense wire gas gain, isochronicity and two track separability. Fig 24 shows that part of the drift cell close to a sense wire in the vertex detectors of MarkII and L3 (the latter is more exotically known as the Time Expansion Chamber). The use of extra sense and field wires improves isochronicity and two track separation by

The D-Zero vertex detector for the Fermilab hadron collider is reported by LOKEN et al. [26] at this conference. The slow gas plus conventional electronics approach is used in a multi-cell jet chamber-like drift device in which three layers of jet cells with a double potential wire plane are staggered in azimuth ϕ (fig 26). There is no need to tilt the drift cells as in the stereo superlayer chambers at CDF and Zeus because D-Zero has no magnetic field. The detector is upstream with respect to the interaction vertex of a TR detector and high precision calorimeter and therefore must be very lightweight so overpressure is not possible. The sense wire spacing of 0.18 inch is mechanically stable and meets the requirements of sufficiently large ionisation sampling in the available space when both a sensible drift field of 1 to 2 kV/cm (drift velocity $\sim 10 \mu\text{m/ns}$) and a gas gain of a few times 10^4 are maintained. The drift cell is sufficiently small to handle the expected occupancy in the high rate environment close to the beam pipe. A prototype test chamber with 1 bar dimethyl ether (DME), another slow gas ($v_{\text{drift}} = 8.3 \mu\text{m/ns}$, $E_{\text{drift}} = 2.3 \text{ kV/cm}$), read out into conventional 100 MHz FADCs, has been tested, and impressive spatial resolution in the drift co-ordinate is obtained (fig 27). An analysis of the efficiency for distinguishing overlapping pulses is also shown and it is concluded that 90% of pulses are separated by more than 84 ns, corresponding to 0.7 mm spatially (fig 27) and arguing well for two track separation in the final device. The chamber will also measure the axial co-ordinate z using both charge division and four layers of cathode pads. The latter are included to compensate for the loss of charge division information on tracks with the same azimuth ϕ .

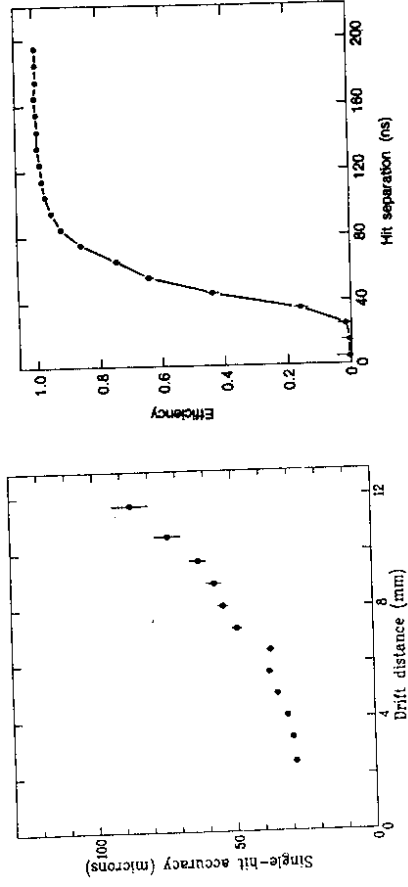


Fig 27. Spatial resolution as a function of drift distance and adjacent hit efficiency in the prototype D-Zero vertex chamber as a function of hit separation in ns; at nominal operating conditions 90% of adjacent hits are resolved for spatial separations $\geq 0.7 \text{ mm}$ [26].

Despite the severe demands of high precision, multi-vertex reconstruction in the dense environment close to the primary interaction vertex at present and future colliders, there has been a continual improvement in techniques of both construction and operation of gaseous drift chambers designed as vertex detectors.

3. The Future

3.1 Developments in High Precision with High Rate Tolerance

At all future hadron colliders there exists a major rate problem for gaseous detectors due both to large cross sections for low P_T physics and to beam halo background close to the interaction vertex. Thus improvements in drift chamber precision, essential for meaningful charged track recognition and reconstruction at the high energy involved, must be developed with high rate in mind. Two notable ideas have so far been tested in small prototypes with some success. Both accommodate the problems of high rate by using small drift volumes so that the charge collection per wire is kept at acceptable levels.

The Induction Drift Chamber (IDC) of WALENTA et al. [27] measures the spatial distribution round the sense wire of the sense wire avalanche in a conventional "MWPC-like" wire geometry (fig 28) by read-out induced signals on adjacent field (potential) wires. The wire plane thus contains alternate field (potential) as well as sense wires. The drift cell electrostatics follow the classic Erskine configuration [28] with no static charge on the field wires and with ionisation drift roughly parallel to the track

isolating the drift region from the avalanche region close to the sense wire, though it must be said that the optimisation helps least those tracks (the majority) which are not perpendicular to the drift direction.

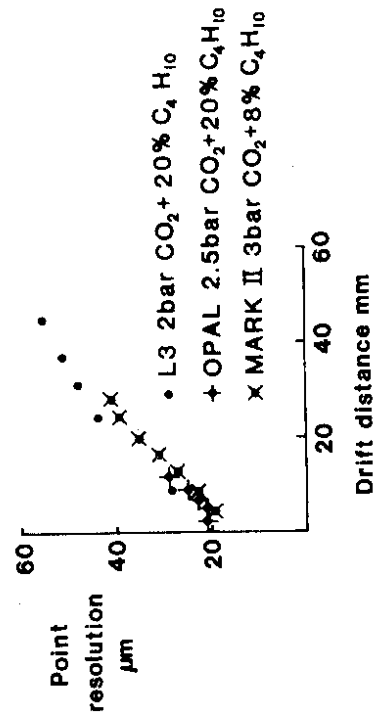


Fig 25 Measurements by the L3, MarkII and OPAL. groups of spatial resolution in pressurised $\text{CO}_2 + i\text{-C}_4\text{H}_{10}$ [25].

In general these LEP vertex chambers are operated with a drift field of $\sim 1.5 \text{ kV/cm}$ bar for which the drift velocity has a linear variation with drift field of $\sim 7.5 (\mu\text{m/ns})/(\text{kV/cm})$. To avoid major systematic effects due to variation of drift velocity over a typical 2 cm drift length, drift field voltage, gas pressure, gas temperature and isobutane content must be known to $\sim 0.03\%$. There is also a problem of low gas gain in this slow gas which means that surface fields have to be larger than is comfortable for easy mechanical stability within the required accuracy of assembly. Nevertheless impressive results are possible in prototypes; fig 25 shows spatial resolution results from L3, OPAL and MarkII in ~ 2 to ~ 3 bar $\text{CO}_2 + i\text{-C}_4\text{H}_{10}$. The alternative is to go for more sophisticated electronics, and thus cost, and a gas with higher gain but greater drift velocity, such as $\text{Ar:C}_2\text{H}_6$ 50:50.

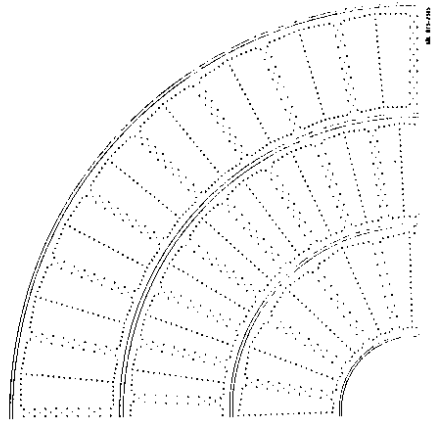


Fig 26. $r-\phi$ view of a quadrant of the D-Zero vertex detector, each of three layers is staggered relative to the others in ϕ ; a double plane of potential wires is used in each cell for improved isochronicity and two-track separation [26].

direction in the usual MWPC configuration. The drift cell dimensions are small to accommodate the high rate specification - sense to sense separation $\leq 600 \mu\text{m}$, sense and field wire to cathode plane spacing wire spacing $\leq 6 \text{ mm}$. The chamber is operated with 1 bar isobutane ($i\text{-C}_4\text{H}_{10}$). Tracks which cross the sense wire plane normally will deposit ionisation which to good approximation drifts along a unique trajectory to the nearest sense wire. The induced signals on field wires sandwiching a sense wire depend on the distance across the drift cell of the incident track ionisation. Thus pulse height on the sense wires and the difference between the induced signals on the potential wires are read-out. There is no timing measurement of ionisation drift.

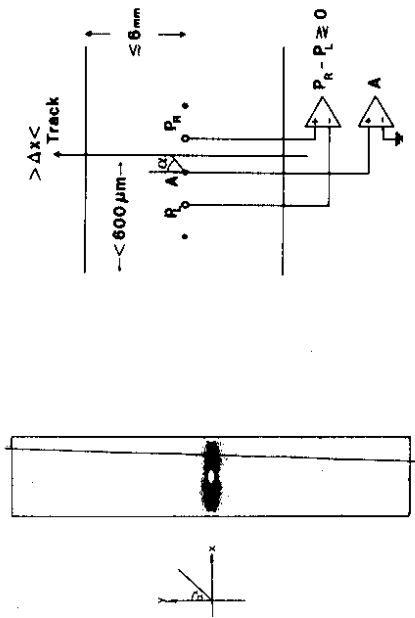


Fig 28. Schematic of operation of the Induction Drift Chamber; the electrostatic map of ionisation drift trajectories is shown together with the read-out scheme using differential amplifiers on both sense and field/potential wires with which the distance Δx of the track from the sense wire is calculated [27].

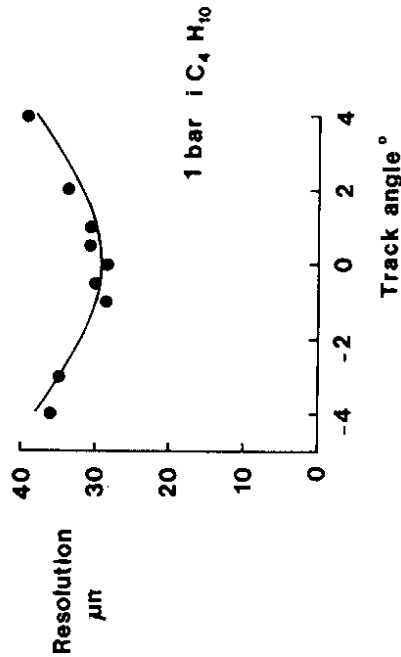


Fig 29 Spatial resolution in a prototype Induction Drift Chamber as a function of the angle of incidence of a track; the gas is $i\text{-C}_4\text{H}_{10}$ at 1 bar [27].

From these data the angle α at which the track ionisation approaches the sense wire avalanche region can be determined, and thus, using the electrostatic simulation (the standard Erskine formula), the distance Δx of the track from the sense wire can be found. The results are impressive and are shown in fig 29. The IDC drift cell is also small and so hopefully can be operated in a fairly high rate environment. However in a real experimental environment cell occupancy may exceed 1 and tracks may be incident at acute angles making it impossible to understand data without some additional spatial

information. Thus whether a large charged track detector which exploits the IDC principle is viable, and how well it will work, when possibly also situated in a substantial magnetic field, is still completely unclear.

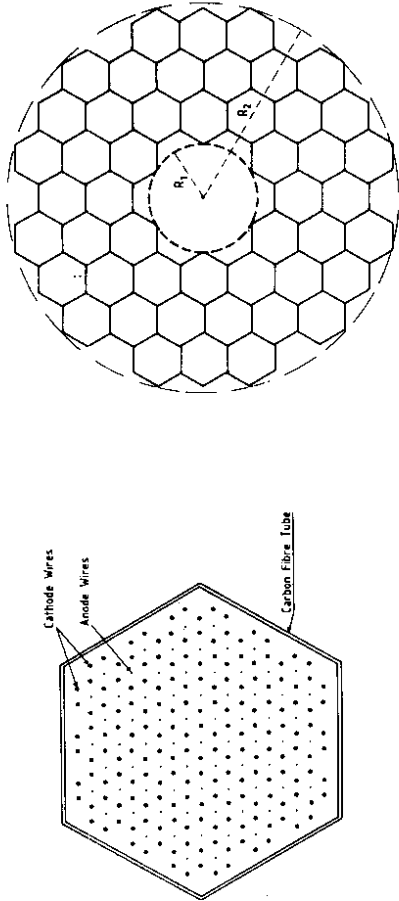


Fig 30. Schematic of assembly of Multi-Drift Module (MDM); a single module is shown as an array of hexagonal drift cells supported in a C-fibre hexagonal tube; also shown is a putative array of MDMs forming a high precision, high rate track detector [29].

An alternative approach is the Multi-Drift Module (MDM) of BOULLIER et al. [29]. Here the problems of high rate are solved by building modules containing very large numbers of sense wires in very small drift cells by means of novel lightweight, high precision structures. Each drift cell in an MDM consists of sense wires surrounded by six cathode wires in a hexagonal matrix structure (fig 30). Then stacks of MDMs are built up round the interaction point providing a very high density of drift cells to disentangle the pattern recognition problems. Each drift cell radius is small, 1.45 mm (1.27 mm between wire planes), and the mechanical support comes from a thin carbon fibre tube 30 mm in diameter. One module thus contains 70 drift cells. Wires are supported on two precision drilled glass fibre plates in V shaped grooves to an overall accuracy of $< 20 \mu\text{m}$. Point resolutions of $\sim 70 \mu\text{m}$ have been achieved in 1 bar DME, which is an encouraging start. The whole detector bears an uncanny resemblance to the multi-cell geometry of, for example, the old TASSO, PLUTO and CELLO central track detectors, though of course the density of drift cells is much larger, their size is much smaller and their point accuracy much greater. One major advantage of the MDM configuration with cylindrical-like drift cells compared with the multi-wire cell devices in the vertex detectors above is that tracks at virtually any angle in the $r\text{-}\phi$ plane still keep the high precision timing measurement. To date the MDM has at least demonstrated that there are no problems of mechanical stability for its large density of wires over 0.8 m length and thus that it does form a most convenient way of assembling a very high density of low mass straw-like chambers. A similar device, based on a "Wellblech" structure in which the hexagonal cells become square and the cathode is a continuous corrugated structure bringing a welcome reduction in the number of wires, has been constructed 1 m long [30].

It remains to be seen how well both the IDC and MDM devices can be exploited in realistic charged track detectors. In particular, the very high density of sense wires implies both mammoth expenditure on present day read-out electronics and another step up in the sophistication of techniques for mechanical construction. Optimistically it is not unreasonable to anticipate that the rate of progress of the last decade will continue and these considerable problems will be solved.

3.2 Tracking at Super-colliders

Proposed future super-colliders come with distinct sets of problems as far as the use of gaseous charged track detectors are concerned, depending on the machine luminosity, the magnitude of the total interaction cross-section, the expected backgrounds and the duty cycle associated with the machine bunch crossing rate. Nevertheless working groups studying the feasibility of charged track detection at LHC (pp, ep), CLIC (e^+e^-) and SSC (pp) have concluded that gaseous charged track detection may again play a crucial role in the physics of this new energy scale [31].

The most severe background problems will come in the hadron super-colliders in which luminosities of $10^{33} \text{ cm}^{-2} \text{ s}^{-1}$ are possible and the total interaction cross-section is huge. Fig 31 shows the estimated radiation levels at SSC (due to everything) - it will be hard to operate close into the interaction vertex. At the e^+e^- linear super-collider (CLIC) problems may not so severe, but they will arise mainly due to the isotropic cloud of multiply scattered soft (KeV) photons generated by the baffles shielding the harder "beamstrahlung" fluxes associated with the colliding bunches. Experience at SLC will be educational.

Table I

HERA	96 ns
LEP	25 μs
SLC	6 to 8 ms
CLIC	170 μs
LHC pp	$\leq 25 \text{ ns}$
ep	165 ns
SSC	25 ns

Bunch Crossing Intervals at Present and Future Colliders

High bunch crossing rates pose complications for drift chamber devices with few microsecond drift times when luminosity and total interaction cross-section mean an event or so per bunch crossing. Table I summarises the between-bunch time intervals of some present machines and proposed super-colliders. LHC therefore poses a major problem for experiments with gaseous detectors. As has already been inferred, drift chamber systems capable of handling 1 or 2 interactions per bunch crossing at HERA have been designed using digital pipelines [16,20]. For the Zeus central drift chamber operating with a first level trigger rate of 10 kHz, the expected dead-time is 0.6%. Similar techniques may be possible at the LHC.

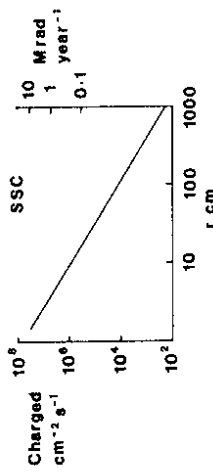


Fig 31 Radiation levels at the SSC as a function of radial distance from the beam pipe [31].

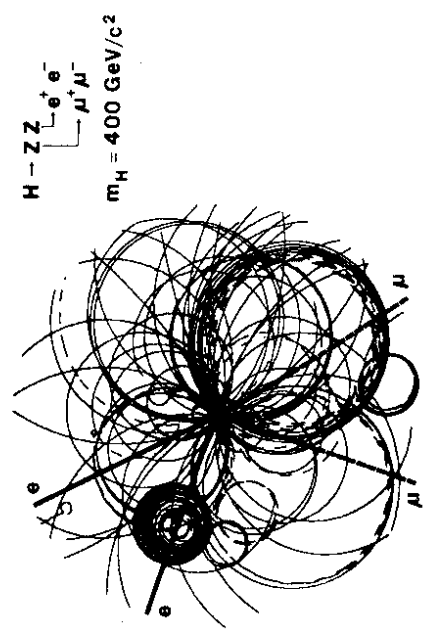


Fig 32. SSC event showing the production of a Higgs boson (mass 400 GeV/c²) and subsequent decay to $e^+e^-\mu^+\mu^-$ via two intermediate Z bosons; the lepton track vectors are marked at the interaction vertex [33].

Jet simulations (1 TeV jet energy) at these new machines suggest that charged track detection by means of detectors with 2 mm minimum track separation is feasible provided the detector is more than about 50 cm from the interaction point [31,32]. Typical charged multiplicity is 80 and broadly spread. 40% of jet energy is carried by particles of 90 GeV/c or more. A momentum resolution of $\sigma(p)/p \sim 0.3$ TeV⁻¹ is sensible criterion for specifying magnetic tracking as it permits the determination of the charge on a 1 TeV track. It then turns out that a track length of 2 m in a field B of 2 T with 150 track points, each with 150 μm accuracy or better, is adequate provided that track-finding is still possible. Recent studies by HANSON et al. have gone further and established that track finding within dense SSC jets is meaningfully possible in a stereo superlayer like device [33]. Moreover in an axial magnetic field the interesting high p_T signal is spread spatially at larger radii and confusion from low p_T contributions is removed. Fig 32 shows a Higgs event in the central detector of an SSC experiment with solenoidal magnetic field; enough track points are found on the lepton tracks for reconstruction despite the confusion of other tracks. Work is continuing on a full pattern recognition.

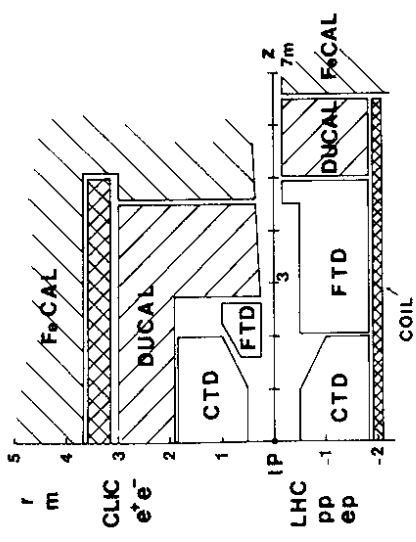


Fig 33. Putative layout of a detector at the SSC, LHC or CLIC showing the arrangement of inner tracking detectors inside a high precision calorimeter system; two arrangements are shown, one with enhanced forward track detection essential for an ep detector [31]

The LHC working group went so far as to propose a vector drift chamber with six super-layers and with an unadventurous space point resolution (150 μm in a decade's hence) for $50 < r < 160 \text{ cm}$ inside a solenoid [31,34]. All estimates suggest that such a chamber would operate for several years in LHC with a gas gain of $\sim 2 \cdot 10^4$. A forward detector in the axial (solenoid) field consisting of stacks of radial drift chambers looks similarly feasible and gains an extra unit of rapidity [31,35]. Fig 32 shows the schematic layout. There is space enough outside a radius of 0.5 m, given the constraints from calorimeter segmentation, for a CTD of outer radius 2 m. Some of the work concerned with small drift cells of very high precision, described in section 3.1 above, may mean that the tracking detectors can be smaller than the volumes required in fig 32 (CTD of ~ 20 to $40 \text{ m}^2 - \text{c f OPAL } 28 \text{ m}^2$). One begins to be encouraged in the belief that gaseous track chambers will form the basis of any multi-track detector at highest energy colliders for the foreseeable future. There are plans to continue these studies in an attempt to arrive at a realistic central track detector at the SSC which may be a hybrid of semi-conductor strips, pixel devices and gaseous drift chambers [33].

4. Conclusion

All present day charged track detectors have to operate in a high multiplicity environment. Gaseous drift chambers form the basis of all such detectors. Their successful use in these hostile environments is a triumphant monument to the immense development work which has taken place over the last decade. The problems faced by experimentation at the next generation of multi-TeV colliders such as SSC and LHC are very much more severe and their implications for gaseous drift chambers are only now being fully grasped. Their solutions will require considerable development, but already it seems realistic to

envisage the gaseous drift chamber as a major part of charged track detection at this new energy scale, that is in even higher multiplicity backgrounds than hitherto encountered.

Acknowledgements

I wish to thank Prof Ch. Fabjan for organising an interesting and stimulating session on detector developments at this conference. I also thank all those who supplied me at short notice with information concerning new developments for this presentation. I remain indebted to many colleagues at Liverpool, DESY, RAL and Aachen, working both on the H1 experiment at HERA and elsewhere, from whom and with whom I have learnt and discovered many of the pitfalls and joys of designing, constructing and testing high precision track detectors. I acknowledge excellent secretarial help in the preparation of this report from Mac Plus.

References

1. J M Gaillard, rapporteur talk in session 22 - these proceedings
C Goessling, rapporteur talk in session 22 - these proceedings
M Turala, rapporteur talk in session 22 - these proceedings
J Va vra, Nucl. Instr. and Meth. **A252** (1986) 547
2. D R Nygren, Proposal to investigate the feasibility of a novel Concept in Particle Detection, LBL Internal Report (1974)
3. D R Nygren, **PEP-198** (1975)
4. Proposal for the PEP4-TPC, **SLAC PUB-5012** (1976)
5. R L Wagner, Nucl. Instr. and Meth. **A265** (1988) 1
6. ALEPH Collaboration Technical Report **CERN/LEPC/83-2** (1983)
7. ALEPH Collaboration Technical Report **CERN/LEPC/84-15** (1984)
8. DELPHI Technical Proposal **CERN/LEPC/83-3** (1983)
9. DELPHI Progress Report **CERN/LEPC/84-16** (1984)
10. Private Communication PEP4-TPC Group (via S J Maxfield)
11. T Kamae, "Results from e⁺e⁻ Collisions", plenary talk in these proceedings
12. S J Lindebaum et al. (Brookhaven, City College of New York, Johns Hopkins, Rice Collaboration), "Development and Tests of an Anode Readout TPC with High Track Separability for large solid angle Relativistic Ion Experiments", paper A471 submitted to this conference, and S J Lindebaum, private communication
13. Yu.a. Budagov et al. (Dubna, Tashkent Collaboration), "Test of Time Projection Chamber Prototype with a Delay Line Read-out", paper 0631C submitted to this conference
14. C Gruhn and CERN NA36 experiment, private communication
15. D H Saxon, Nucl. Instr. and Meth. **A265** (1988) 20
16. R D Heuer and A Wagner, Nucl. Instr. and Meth. **A265** (1988) 11
17. J Roehrig et al, Nucl. Instr. and Meth. **226** (1984) 319
18. G Hanson, Nucl. Instr. and Meth. **A252** (1986) 343
19. Zeus Technical Proposal, DESY, March 1986
20. Zeus Technical Progress Report, DESY, September 1987
21. N Hamew, private communication
22. S Biagi and P S L Booth, Nucl. Instr. and Meth. **A252** (1986) 586;
23. comparator electronics (CMOS technology) with 0.5 ns timing bins (~80 ps edge slewing) is now implemented on the DELPHI Outer Detector, P S L Booth, private communication
24. G Bertrand-Coremans et al., "The Central Tracking System of the H1 Experiment", paper A216 submitted to this conference
25. H1 Technical Proposal, DESY, March 1986
26. H1 Technical Progress Report, DESY, September 1987
27. P R Burchat et al., **SLAC-PUB-3475** (1984)
28. SLD Design Report, **SLAC-Report-273** (1984)
29. W B Atwood et al., Nucl. Instr. and Meth. **A252** (1986) 295
30. H Grassler et al., "Simultaneous Track Reconstruction and Electron Identification in the H1 Forward Track Detector", poster session at this conference.
31. M Atac et al., IEEE Trans on Nuclear Science **NS-32** No. 1 (1985) 595
32. K G Hayes, Nucl. Instr. and Meth. **A265** (1988) 60 and references therein
33. J Alexander et al. (MarkII vertex detector), Nucl. Instr. and Meth. **A252** (1986) 350
34. H Anderhub et al. (Time Expansion Chamber), Nucl. Instr. and Meth. **A252** (1986) 357

26. S C Loken et al., "The D-Zero Drift Chamber Vertex Chamber", paper A460C submitted to this conference
A R Clarke et al., Nucl. Instr. and Meth. **A261** (1987) 420
A H Walenta et al., Nucl. Instr. and Meth. **A265** (1988) 69 and references therein
27. G A Erskine, Nucl. Instr. and Meth. **105** (1972) 565
28. M Tonutti et al., Proceedings of the Workshop on Physics at Future Accelerators, La Thuile (Italy) and Geneva (Switzerland), ed J H Mulvey, **CERN 87-07 Vol. II** (1987) 494
29. Report of the Task Force on Detector R and D for the SSC, **SSC-SR-1021** (1986)
30. D H Saxon, Summary Report of working Group on Vertex Detection and Tracking, Proceedings of the Workshop on Physics at Future Accelerators, La Thuile (Italy) and Geneva (Switzerland), ed J H Mulvey, **CERN 87-07 Vol. I** (1987) 205
31. P N Burrows and G Ingelman, Proceedings of the Workshop on Physics at Future Accelerators, La Thuile (Italy) and Geneva (Switzerland), ed J H Mulvey, **CERN 87-07 Vol. I** (1987) 369
32. G Hanson, B Niczyporuk and A Palounek, Proceedings of the Conference on Future Directions in Detector R&D for Experiments at pp Colliders, July 5-7th 1988, Snowmass (USA), in litt., and G Hanson, private communication.
33. E Eisen and A Wagner, Proceedings of the Workshop on Physics at Future Accelerators, La Thuile (Italy) and Geneva (Switzerland), ed J H Mulvey, **CERN 87-07 Vol. II** (1987) 463
34. J B Dainton, Proceedings of the Workshop on Physics at Future Accelerators, La Thuile (Italy) and Geneva (Switzerland), ed J H Mulvey, **CERN 87-07 Vol. II** (1987) 478